Majorana bound states and non-local spin correlations in a quantum wire on an unconventional superconductor

Sho Nakosai,[1] Jan Carl Budich,[2] Yukio Tanaka,[3] Björn Trauzettel,[4] and Naoto Nagaosa[1,5,6]

[1]*Department of Applied Physics, University of Tokyo, Tokyo 113-8656, Japan*
[2]*Department of Physics, Stockholm University, Se-106 91 Stockholm, Sweden*
[3]*Department of Applied Physics, Nagoya University, Aichi 464-8603, Japan*
[4]*Institute for Theoretical Physics and Astrophysics, University of Würzburg, 97074 Würzburg, Germany*
[5]*Correlated Electron Research Group (CERG), RIKEN Advanced Science Institute (ASI), Wako 351-0198, Japan*
[6]*Cross-Correlated Materials Research Group (CMRG), RIKEN Advanced Science Institute (ASI), Wako 351-0198, Japan*

(Dated: November 13, 2012)

We study theoretically the proximity effect of a one-dimensional metallic quantum wire (in the absence of spin-orbit interaction) lying on top of an unconventional superconductor. Three different material classes are considered as a substrate: (i) a chiral superconductor in class D with broken time-reversal symmetry; a class DIII superconductor (ii) with and (iii) without a nontrivial $\mathbb{Z}_2$ number. Interestingly, we find degenerate zero energy Majorana bound states at both ends of the wire for all three cases. They are unstable against spin-orbit interaction in case (i) while they are topologically protected by time-reversal symmetry in cases (ii) and (iii). Remarkably, we show that non-local spin correlations between the two ends of the wire can be simply controlled by a gate potential in our setup.

PACS numbers: 74.45+c, 74.20.Rp

Introduction.– Proximity effects of superconductors and normal metals as well as semiconductors have been a subject of continued interest due to the rich physical phenomena of these hybrid systems. Especially, the topological nature of the superconducting proximity effect is an issue of current research activities [1–4] stimulated by the possible occurrence of Majorana fermions in solid state systems [5–11]. For example, the interface between an s-wave superconductor and the surface state of a three-dimensional topological insulator (TI) is predicted to offer a platform to realize Majorana fermions [1]. The underlying idea here is holographic principle that entails the reduction of electronic degrees of freedom, i.e., electron fractionalization, at the surface of a topologically non-trivial bulk state. Furthermore, the proximity effect of a TI to unconventional superconductors has also been studied theoretically [12]. Another (highly interesting) proposal is to use semiconductors with Rashba spin-orbit interaction in combination with s-wave superconductors for this purpose. In the presence of a sufficiently strong magnetic field, an inverted gap opens at the Γ-point in this system and topological superconductivity as well as Majorana fermions may appear when the Fermi energy lies inside the gap [13–16]. A recent experiment observed the zero-bias conductance peak at the edge of an InSb quantum wire (QW) coupled to an s-wave superconducting substrate, which might be the first experimental observation of a Majorana fermion [17]. It has also been shown theoretically that a one-dimensional Rashba quantum wire coupled to a d-wave superconductor hosts doubly degenerate Majorana bound states (MBSs) at the edge [18]. Besides these distinct works, there are various other research activities on the basis of QWs (for example Refs. [16, 19–25]). In all the cases listed above, spin-orbit interaction and/or the Zeeman energy in the QW is essential. Therefore, an open question is if zero energy Majorana bound states are also realizable in a one-dimensional system in the absence of these interactions, which opens new opportunities as we will show below.

In this paper, we investigate electronic states caused by the proximity effect between a metallic QW and a two-dimensional (2D) unconventional superconductor to search for zero energy MBSs at the ends of the QW. We discover that the resulting MBSs are doubly degenerate, i.e., characterized by a spin degree of freedom. This leads to nonlocal spin-correlations between the two ends of the QW which can be manipulated by all-electric means. For a substrate in symmetry class D [26], i.e., in the absence of time reversal symmetry (TRS) the degenerate end states can be gapped out by switching on TRS preserving local imperfections that couple opposite spin. This is reflected in the fact these systems are characterized by a trivial $\mathbb{Z}_2$ topological invariant. In contrast, for a TRS preserving substrate in symmetry class DIII, we find helical MBS pairs that are topologically protected by TRS.

Model.– Our setup is shown schematically in Fig. 1 and the model Hamiltonian given by

$$H_{\rm SC} = \int {\rm d}^2 k \Psi^\dagger_{\boldsymbol{k}} \begin{pmatrix} \frac{k_x^2+k_y^2}{2m_s} - \mu_s & \hat{\Delta} \\ \hat{\Delta}^\dagger & -\frac{k_x^2+k_y^2}{2m_s} + \mu_s \end{pmatrix} \Psi_{\boldsymbol{k}}, \quad (1)$$

$$\Psi_{\boldsymbol{k}} = \left(a_{\uparrow \boldsymbol{k}} \; a_{\downarrow \boldsymbol{k}} \; a^\dagger_{\uparrow -\boldsymbol{k}} \; a^\dagger_{\downarrow -\boldsymbol{k}} \right), \quad (2)$$

$$H_{\rm wire} = \int {\rm d}k \psi^\dagger_{\sigma k} \left[\frac{k_x^2}{2m} - \mu \right] \psi_{\sigma k}, \quad (3)$$

$$H_{\rm t} = c \int {\rm d}x \left(\psi^\dagger_{x\sigma} a_{(x,0)\sigma} + {\rm h.c.} \right), \quad (4)$$

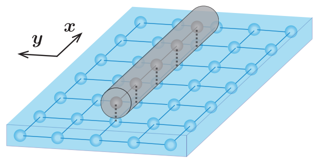

FIG. 1. One dimensional metallic quantum wire (QW) on top of a substrate of an unconventional two dimensional SC. The wire is located along the x axis. Dashed lines illustrate tunneling between the QW and the SC, and solid spheres represent the sites of our tight-binding model discussed in the text.

where $H_{\rm wire}$ describes the QW put along x-direction on the surface of the superconductor described by $H_{\rm SC}$ which infinitely spreads in the xy-plane. These two are connected by a tunneling Hamiltonian $H_{\rm t}$ with the spin-independent constant matrix element c. We consider the following three cases for the order parameter matrix $\hat{\Delta}$: (i) $\hat{\Delta} = i\sigma_y\Delta\sigma_z(k_x + ik_y)$ for the chiral superconductor of class D with the topological invariant $Z = 1$, and (ii) $\hat{\Delta} = i\sigma_y\Delta\boldsymbol{k}\cdot\boldsymbol{\sigma}$ for the time reversal symmetric class DIII superconductor with the topological invariant $\mathbb{Z}_2 = 1$. Here, the σ denotes Pauli matrices in spin space. As the third case (iii), we consider a system where two layers of a 2D superconductor of case (ii) are coupled to each other by an interlayer transfer integral, which is a topologically trivial case with $\mathbb{Z}_2 = 0$. The model (i) is relevant to Sr_2RuO_4 where the chiral $p + ip$ superconductivity with broken time-reversal symmetry is believed to be realized [27]. The model (ii) is the 2D analogue of the He B phase, and is continuously connected to the helical non-centrosymmetric topological superconductor with Rashba spin-orbit interaction [28–30]. We present the calculational steps and results mainly for case (i) below, but it is straightforward to apply them to the other two cases (ii) and (iii). Our main purpose is to investigate the electronic states in the one-dimensional superconductivity formed in this way and to discuss its topological nature as well as resulting Majorana bound states.

Effective Green's function.– First, we derive the effective Green's function of the QW by integrating over the superconductor

$$G_{\rm eff}^{-1}(i\omega_n, k_x) = i\omega_n - H_{\rm wire}(k_x)\tau_z - c^2 I(i\omega, k_x), \quad (5)$$

$$I(i\omega_n, k_x) = \int {\rm d}k_y \frac{i\omega_n + H_{\rm SC}(k_x, k_y)}{(i\omega_n)^2 - H_{\rm SC}^2(k_x, k_y)}, \quad (6)$$

where τ denotes Pauli matrices in the Nambu space. As long as there is neither spin-orbit interaction in the wire nor spin-dependent tunneling between the wire and the superconductor, theinduced superconducting order parameter is also spin-triplet and can be decoupled into two sectors $\sigma_x = \pm 1$. The

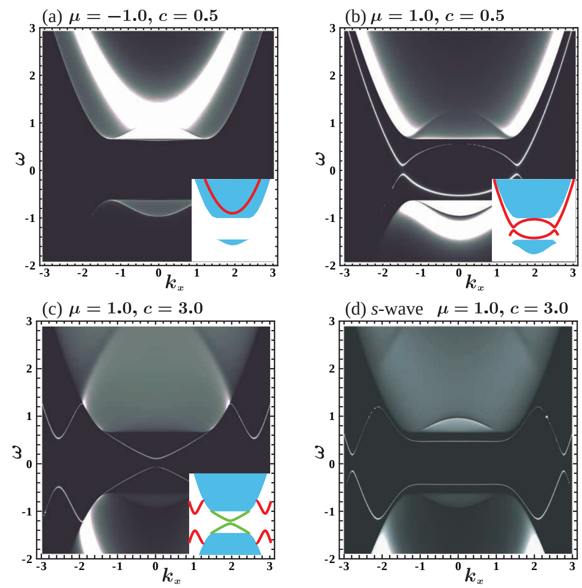

FIG. 2. Spectral function of the electronic excitations. The insets show the schematic structure of the spectrum; Blue: continuum of the substrate superconductor, Red: 1D states of the QW, and Green: edge states of the 2D SC induced by the coupling to the QW. In (a) the states in the QW are located outside the superconducting gap, while in (b) these states are within the superconducting gap and an SC order parameter is induced in the QW. (c) is the case where the coupling is strong enough that the bonding and anti-bonding states act as a potential barrier and edge states in the 2D superconductor emerge. (d) shows that no zero energy states are formed in an s-wave superconductor under the same conditions as (c).

integration can be analytically performed and we obtain

$$G_{\rm eff}^{-1}(i\omega_n, k_x) = i\omega_n(1 - 2c^2 I_1) - \boldsymbol{h}(k_x)\cdot\boldsymbol{\tau}, \quad (7)$$

$$\boldsymbol{h}(k_x) = \left(2c^2\Delta k_x I_1\sigma_x,\ 0,\ \xi_k + 2c^2\xi_k^{\rm SC} I_1 + 2c^2 I_2\right), \quad (8)$$

$$I_1 = \frac{m_{\rm s}\left[\lambda_+^{-1}\arctan\left(\kappa/\lambda_+\right) - \lambda_-^{-1}\arctan\left(\kappa/\lambda_-\right)\right]}{2\pi\sqrt{m_{\rm s}^2\Delta^4 - 2m_{\rm s}\Delta^2\mu_{\rm s} - \omega_n^2}}, \quad (9)$$

$$I_2 = \frac{\lambda_-\arctan\left(\kappa/\lambda_-\right) - \lambda_+\arctan\left(\kappa/\lambda_+\right)}{4\pi\sqrt{m_{\rm s}^2\Delta^4 - 2m_{\rm s}\Delta^2\mu_{\rm s} - \omega_n^2}}, \quad (10)$$

where κ is a momentum cut-off and $\lambda_\pm = \left(k_x^2 + 2m_{\rm s}^2\Delta^2 - 2m_{\rm s}\mu_{\rm s} \pm 2m_{\rm s}\sqrt{m_{\rm s}^2\Delta^4 - 2m_{\rm s}\Delta^2\mu_{\rm s} - \omega_n^2}\right)^{1/2}$, $\xi_k = k^2/2m - \mu$, $\xi_k^{\rm SC}$ likewise. In the following, we look at the $\sigma_x = 1$ sector, which is equivalent to a spinless p-wave superconductor. From Eq. (8), we can then calculate the spectral function $A(\omega, k_x)$ of the electron as

$$A(\omega, k_x) = -\frac{1}{2\pi}\Im\left[{\rm Tr}\left[\tau_z G_{\rm eff}^{\rm R}(\omega, k_x)\right]\right], \quad (11)$$

where $G_{\rm eff}^{\rm R}(\omega, k_x)$ is the retarded Green's function obtained from $G_{\rm eff}(i\omega_n, k_x)$ via the analytic continuation $i\omega_n \to \omega + i\delta$, where δ is a infinitesimally small positive number. In Fig. 2, we plot Eq. (11) with $m = m_s = 1.0$, $\mu_s = 1.0$, $\Delta =$

0.5, and several values of μ and c. The insets show the schematic structure of the spectrum. The red lines represent states in the wire without and with an induced superconducting gap, in cases (a) and (b) respectively. The blue shaded area shows the continuum of the bulk states in the superconductor, which arises in the effective Green's function of the QW as the self-energy (Eqs. (5) and (6)). The green lines are edge states in the 2D SC that will be further discussed below. Figures 2(a) and (b) correspond to the cases where the band of the QW is outside and inside of the superconducting gap of the substrate superconductor, respectively. We can see that in Fig. 2(b) a finite gap is induced by the proximity effect. An interesting situation arises when the magnitude of the transfer integral related to the tunneling c is strong enough that bonding and anti-bonding states are formed at the interface of the wire and the superconductor. The energy of those states is pushed away from the low energy regime, and they act as a potential barrier to other states. Therefore, a boundary is effectively induced in the substrate superconductor. It is known that edge modes appear at the boundary of 2D topological superconductors. The energy of the midgap states around $k_x = 0$ approach zero as the magnitude of c becomes larger (see Fig. 2(c)). This shows the formation of edge channel that are gapped out because the edge modes located at both sides of the wire weakly interact with each other. In Fig. 2(d) we show the spectral function for an s-wave superconductor substrate for comparison. There are no states corresponding to the edge channel in case (c).

Topological nature.– Now, we focus on the topological nature of the QW system. For this purpose, we use the method for the calculation of the topological number in terms of Green's function at zero frequency [31, 32]. We derive an effective Hamiltonian from Eq. (5) on the basis of $H_{\rm eff}(k_x) = -G^{-1}_{\rm eff}(i\omega_n = 0, k_x) = \boldsymbol{h}(k_x) \cdot \boldsymbol{\tau}$ for a given $\sigma_x = \pm 1$. This 2×2 Hamiltonian is similar to that of Kitaev's original proposal of a 1D topological superconductor [33]. It is known that the system is in the topological phase when $\hat{\boldsymbol{h}}(k_x) = \boldsymbol{h}/|\boldsymbol{h}|$ connects antipodal points of the unit sphere as k_x is varied from the center to the boundary of the Brillouin zone [4]. Therefore, it is easy to verify that when $\mu > 2c^2(-\mu_{\rm s} I_1(k_x = 0) + I_2(k_x = 0)) = \mu^*$, the QW becomes two copies of Kitaev's 1D topological superconductor with $\mathbb{Z}_2 = 1$. The topological nature of the 1D superconductor manifests itself in bound states at the ends of the QW, which will benumerically studied in the following. However, in case (i), the two identical copies of the $\mathbb{Z}_2$-nontrivial Kitaev model form a trivial composite system. Physically, this implies that the degenerate end states can be gapped out by switching on terms that couple the opposite spin sectors as we confirmed by numerical calculations.

Numerical study of a tight-binding model and Majorana bound states.- We study a tight-binding model by numerical calculations. We change our continuum model to a lattice model, i.e., $k \to \sin k$ and $k^2 \to 2(1-\cos k)$ in Eq. (8), and construct the corresponding tight-binding Hamiltonian. Then, we calculate the energy spectrum in the system with *open boundary conditions* as depicted in Fig. 1. Figure 3(a) shows the topological phase transition as a function of the chemical potential in the QW. In the strong coupling regime, where $\mu < \mu^*$, there are no states in the induced superconducting gap, while in the weak coupling regime, where $\mu > \mu^*$ there are zero energy states. It can be checked that four-fold degenerate zero energy states are formed, two at each end. Fig. 3(b) shows the probability distributions of one of them. Red solid circles represent the weight in the QW, and we can see the state is localized at the ends of the wire. In sharp contrast to the Kitaev model, we have two spin sectors in the QW which are degenerate. This fact attaches a spin degree of freedom to the MBSs. However, in the presence of spin-orbit interaction, which mixes the $\sigma_x = \pm 1$ sectors, the degeneracy is lifted and the Majorana fermions will be pushed away from zero energy.

In the following, we briefly discuss the other two possibilities (ii) and (iii) for the SC substrate. We have confirmed that a similar analysis to case (i) outlined above applies to these cases, and we have found that the doubly degenerate zero energy Majorana bound states appear when the chemical potential μ of the QW is positive and large enough for the topological phase transition to occur. In cases (ii) and (iii), the spin degenerate pair of MBS stems from a non-trivial $\mathbb{Z}_2$ invariant for the composite system in symmetry class DIII. Therefore, these end states are topologically protected by TRS and cannot be gapped out by switching on spin-orbit interaction as long as the bulk gap is maintained. This is an essential difference to case (i) where the conservation of $\sigma_x = \pm 1$ was needed in addition to the generic symmetries of the model to obtain zero energy MBSs, while TRS protects the doubly degenerate MBSs in cases (ii) and (iii). This is particularly remarkable for case (iii) where the substrate 2D superconductor is originally in a topologically trivial phase.

Local and non-local fermions.– There have been many theoretical proposals to use chiral MBSs for topological quantum computing [34–36]. Chiral MBSs are difficult to detect and to manipulate because they only couple in a limited way to their environment. This is different in our proposal. On the one hand, the doubly degenerate MBSs discussed above are more susceptible regarding their coupling to the environment. On the other hand, they can show novel responses through a strong coupling between the fermion parity and the spin degree of freedom. The idea behind is schematically shown in Fig. 4. The solid lines represent Kitaev chains with MBSs indicated by red circles. Let us elaborate a bit more on the two kinds of fermions that can be formed by our MBSs. Since Majorana fermions are real, normal fermions are formed from pairs of them. We can construct two kinds of normal (complex) fermions, *non-local* spin polarized ones $\psi_\uparrow = 1/2(\gamma_{\uparrow 1} + i\gamma_{\uparrow 2})$ and $\psi_\downarrow = 1/2(\gamma_{\downarrow 1} - i\gamma_{\downarrow 2})$, and *local* ones $\psi_1 = 1/2(\gamma_{\uparrow 1} + i\gamma_{\downarrow 1})$ and $\psi_2 = 1/2(\gamma_{\uparrow 2} - i\gamma_{\downarrow 2})$. The local pseudo spin operators are defined as $\boldsymbol{s}_{1(2)} = 1/2 \times \gamma_{1(2)\alpha}\boldsymbol{\sigma}_{\alpha\beta}\gamma_{1(2)\beta}$. It is known that Majorana fermions have only Ising-type spin due to their anticommutation relation $\{\gamma_i, \gamma_j\} = 2\delta_{ij}$, then, $s_x = s_z = 0$ and $s_y = 1/2 - \psi^\dagger\psi$ from the above definition. We would like to emphasize that these local variables are specific to the paired Majorana states.

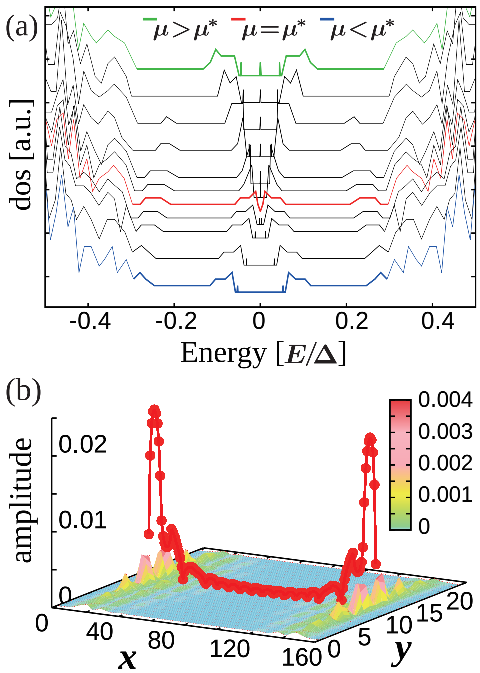

FIG. 3. (a) Density of states with different values of μ. The horizontal axis is in units of the substrate superconducting gap Δ. This plot shows the topological phase transition at $\mu = \mu^*$. There are no states inside the gap when $\mu < \mu^*$ while there are four-fold degenerate zero energy states when $\mu > \mu^*$. (b) Probability distribution of the zero energy states. The size of system is 160×24 for the substrate and 140×1 for the wire. Red solid circles show the probability distribution in the wire, which has peaks at both ends.

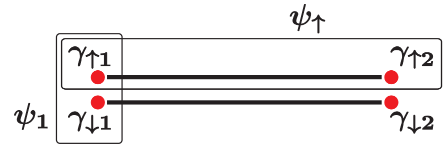

FIG. 4. Schematic figure of Majorana states at the ends of the wire (red circles). As discussed in the main text, the QW can be regarded as two copies of Kitaev model (solid lines). There are two ways to combine two of them into ordinary fermions: *non-local* and *local* ones.

There will be various interesting physics as a consequence of the synthesis of the local and the non-local nature. Here, as an example, we focus on spin-spin correlation of two Ising spins formed at the ends. In preparation for that, we first review some aspects of the fermion parity. When we have two Majorana operators, γ and γ', there exist two orthogonal states $|0\rangle$ and $|1\rangle$, which satisfy $-i\gamma\gamma'|0\rangle = |0\rangle$ and $-i\gamma\gamma'|1\rangle = -|1\rangle$, respectively. The former has an even fermion parity and the latter odd. They can be rewritten by normal fermion operators defined as $\psi = 1/2(\gamma + i\gamma')$ where $\psi^\dagger\psi|0\rangle = 0$ and $\psi^\dagger\psi|1\rangle = |1\rangle$. Note that if the wire is connected to ground by a capacitor, one can modify the fermion number via charging energy $U(n) = Q^2/(2C) - V(t)Q = (Q - Q_0)^2/(2C) + \text{const.}$ where $Q = ne$ is the charge, $V(t)$ is the gate voltage, and $Q_0 = CV(t)$. The importance of charging energy in the context of topological superconductors was first discussed in Ref. [37], where electron teleportation (mediated by the non-locality of the MBSs) has been proposed. We now apply this idea to our model. Our Hilbert space is 4-dimensional and there are two kinds of bases one can construct, i.e., from ψ_1, ψ_2, or from $\psi_\uparrow$, and $\psi_\downarrow$. Namely, one can define $\psi_1^\dagger\psi_1|1\rangle_1 = |1\rangle_1$, *etc.*, and $|0\rangle_1$, $|1\rangle_1$, ... are local basis states while $|0\rangle_\uparrow$, $|1\rangle_\uparrow$, ... are non-local basis states. The relation between these two kinds of basis states is given by

$$\begin{pmatrix} |0\rangle_\uparrow|0\rangle_\downarrow \\ |0\rangle_\uparrow|1\rangle_\downarrow \\ |1\rangle_\uparrow|0\rangle_\downarrow \\ |1\rangle_\uparrow|1\rangle_\downarrow \end{pmatrix} = \frac{1}{\sqrt{2}} \begin{pmatrix} 0 & -i & 1 & 0 \\ 1 & 0 & 0 & i \\ 1 & 0 & 0 & -i \\ 0 & i & 1 & 0 \end{pmatrix} \begin{pmatrix} |0\rangle_1|0\rangle_2 \\ |0\rangle_1|1\rangle_2 \\ |1\rangle_1|0\rangle_2 \\ |1\rangle_1|1\rangle_2 \end{pmatrix} . \qquad (12)$$

In our system, the total number of fermions can be controlled by the gate voltage $V(t)$. We consider $s_1 s_2$ correlation in the odd and even fermion number space, respectively. The density matrices are $\rho_{\text{odd}} = \frac{1}{2}\left(|1\rangle_1|0\rangle_{21}\langle 0|_2\langle 1| + |0\rangle_1|1\rangle_{21}\langle 1|_2\langle 0|\right)$ and $\rho_{\text{even}} = \frac{1}{2}\left(|0\rangle_1|0\rangle_{21}\langle 0|_2\langle 0| + |1\rangle_1|1\rangle_{21}\langle 1|_2\langle 1|\right)$. Then we obtain

$$-\langle s_{1y}s_{2y}\rangle_{\text{odd}} = \langle s_{1y}s_{2y}\rangle_{\text{even}} = \frac{1}{4} , \qquad (13)$$

where $\langle \dots \rangle_{\text{odd/even}}$ represents the statistical average with the density matrices ρ_{odd} and ρ_{even}, respectively. These results show that by modulating charging energy we can control spin-spin correlation, which is independent of the distance between the two spins because they are connected through the superconducting wire in between. This effect is a consequence of both, the local and the non-local degrees of freedom of the system. One can also manipulate the two Ising spins by modulating the gate voltage as a function of time as $V(t) = V_0 + \delta V(t)$. The equations of motion of s_{1y} and s_{2y} by the driving force $\delta V(t)(i\gamma_{1\uparrow}\gamma_{2\uparrow} + i\gamma_{1\downarrow}\gamma_{2\downarrow})$ yield

$$\frac{\mathrm{d}}{\mathrm{d}t}(s_{1y} + s_{2y}) = 0 \qquad (14)$$

$$\frac{\mathrm{d}^2}{\mathrm{d}^2 t}(s_{1y} - s_{2y}) = -4\left(\frac{2e\delta V_0}{\hbar}\right)^2 (s_{1y} - s_{2y}) \qquad (15)$$

for a constant δV_0 during some time period T. By tuning T to satisfy $4e\delta V_0 T/\hbar = \pi$ one can reverse the pseudospins s_y components when they are anti-parallel while they remain unchanged when they are parallel.

Conclusion.– In this paper, we have studied theoretically the proximity effect of a one-dimensional metallic quantum wire without spin-orbit interaction on the substrate of an unconventional superconductor. We have considered three different cases for the substrate: (i) a chiral superconductor; (ii)

a class DIII superconductor with a non-trivial $\mathbb{Z}_2$ number, and (iii) a class DIII superconductor with a trivial $\mathbb{Z}_2$ number. Interestingly, we have found degenerate zero energy Majorana bound states at both ends of the quantum wire for all three cases. We have shown that these degenerate Majorana bound states for cases (ii) and (iii) can be nicely used for a combined spin/parity qubit. Furthermore, we have demonstrated that the resulting non-local spin correlations between the two ends of the wire can be controlled by the gate voltage potential acting on the wire. One of the candidate systems for the case (ii) substrate are thin films of Sr_2RuO_4 [38] or bi-layer Rashba system [30], where the class DIII superconducting state might be realized, and for the case (iii) super lattice structure of $CeCoIn_5$ [39].

Acknowledgment.-SN was supported by Grant-in-Aid for JSPS Fellows and JCB by the Swedish Research Council. This work was further supported by Grant-in-Aid for Scientific Research (S) (Grants No. 24224009) from the Ministry of Education, Culture, Sports, Science and Technology of Japan, Strategic International Cooperative Program (Joint Research Type) from Japan Science and Technology Agency, Funding Program for World-Leading Innovative RD on Science and Technology (FIRST Program), the Deutsche Forschungsgemeinschaft, the European Science Foundation, and the Helmholtz Foundation.

[1] L. Fu and C. L. Kane, Phys. Rev. Lett. **100**, 096407 (2008).
[2] C. W. J. Beenakker, arXiv:1112.1950 (2011).
[3] Y. Tanaka, M. Sato, and N. Nagaosa, J. Phys. Soc. Jpn. **81**, 011013 (2012).
[4] J. Alicea, Rep. Prog. Phys. **75**, 076501 (2012).
[5] E. Majorana, Nuovo Cimento **14**, 171 (1937).
[6] F. Wilczek, Nature Phys. **5**, 614 (2009).
[7] M. Franz, Physics **3**, 24 (2010).
[8] N. Read and D. Green, Phys. Rev. B **61**, 10267 (2000).
[9] D. A. Ivanov, Phys. Rev. Lett. **86**, 268 (2001).
[10] S. Das Sarma, M. Freedman, and C. Nayak, Phys. Rev. Lett. **94**, 166802 (2005).
[11] C. Nayak, S. H. Simon, A. Stern, M. Freedman, and S. Das Sarma, Rev. Mod. Phys. **80**, 1083 (2008).
[12] J. Linder, Y. Tanaka, T. Yokoyama, A. Sudbø, and N. Nagaosa, Phys. Rev. Lett. **104**, 067001 (2010).
[13] M. Sato, Y. Takahashi, and S. Fujimoto, Phys. Rev. Lett. **103**, 020401 (2009).
[14] J. D. Sau, R. M. Lutchyn, S. Tewari, and S. Das Sarma, Phys. Rev. Lett. **104**, 040502 (2010).
[15] J. Alicea, Phys. Rev. B **81**, 125318 (2010).
[16] Y. Oreg, G. Refael, and F. von Oppen, Phys. Rev. Lett. **105**, 177002 (2010).
[17] V. Mourik, K. Zuo, S. M. Frolov, S. R. Plissard, E. P. A. M. Bakkers, and L. P. Kouwenhoven, Science **336**, 1003 (2012).
[18] L. M. Wong and K. T. Law, arXiv:1211.0338 (2012).
[19] J. D. Sau, S. Tewari, R. M. Lutchyn, T. D. Stanescu, and S. Das Sarma, Phys. Rev. B **82**, 214509 (2010).
[20] R. M. Lutchyn, J. D. Sau, and S. Das Sarma, Phys. Rev. Lett. **105**, 077001 (2010).
[21] A. C. Potter and P. A. Lee, Phys. Rev. B **83**, 094525 (2011).
[22] S. Tewari, T. D. Stanescu, J. D. Sau, and S. D. Sarma, New J. Phys. **13**, 065004 (2011).
[23] T. D. Stanescu, R. M. Lutchyn, and S. Das Sarma, Phys. Rev. B **84**, 144522 (2011).
[24] R. M. Lutchyn, T. D. Stanescu, and S. Das Sarma, Phys. Rev. Lett. **106**, 127001 (2011).
[25] Y. Kim, J. Cano, and C. Nayak, arXiv:1208.3701 (2012).
[26] A. P. Schnyder, S. Ryu, A. Furusaki, and A. W. W. Ludwig, Phys. Rev. B **78**, 195125 (2008); S. Ryu, A. P. Schnyder, A. Furusaki, and A. W. W. Ludwig, New J. Phys. **12**, 065010 (2010).
[27] A. P. Mackenzie and Y. Maeno, Rev. Mod. Phys. **75**, 657 (2003).
[28] Y. Tanaka, T. Yokoyama, A. V. Balatsky, and N. Nagaosa, Phys. Rev. B **79**, 060505 (2009).
[29] M. Sato and S. Fujimoto, Phys. Rev. B **79**, 094504 (2009).
[30] S. Nakosai, Y. Tanaka, and N. Nagaosa, Phys. Rev. Lett. **108**, 147003 (2012).
[31] Z. Wang and S.-C. Zhang, Phys. Rev. X **2**, 031008 (2012).
[32] J. C. Budich and B. Trauzettel, arXiv:1207.1104 (2012).
[33] A. Y. Kitaev, Phys.-Usp. **44**, 131 (2001).
[34] J. D. Sau, D. J. Clarke, and S. Tewari, Phys. Rev. B **84**, 094505 (2011).
[35] J. D. Sau, B. I. Halperin, K. Flensberg, and S. Das Sarma, Phys. Rev. B **84**, 144509 (2011).
[36] B. I. Halperin, Y. Oreg, A. Stern, G. Refael, J. Alicea, and F. von Oppen, Phys. Rev. B **85**, 144501 (2012).
[37] L. Fu, Phys. Rev. Lett. **104**, 056402 (2010).
[38] Y. Tada, N. Kawakami, and S. Fujimoto, New J. Phys. **11**, 055070 (2009).
[39] Y. Mizukami, H. Shishido, T. Shibauchi, M. Shimozawa, S. Yasumoto, D. Watanabe, M. Yamashita, H. Ikeda, T. Terashima, H. Kontani, and Y. Matsuda, Nature Phys. **7**, 849 (2011).